Publishing House
AKAPIT

COMPUTER METHODS IN MATERIALS SCIENCE
Informatyka w Technologii Materiałów

Vol. 18, 2018, No. 3

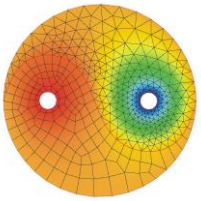

NUMERICAL ANALYSIS OF DAMAGE DURING HOT FORMING

JOANNA SZYNDLER[1,2*], MUHAMMAD IMRAN[1], MUHAMMAD JUNAID AFZAL[1], MARKUS BAMBACH[1]

[1]Brandenburg University of Technology Cottbus-Senftenberg, Konrad-Wachsmann-Allee 17, D-03046 Cottbus, Germany
[2]AGH University of Science and Technology, al. Mickiewicza 30, 30-059 Krakow, Poland
[*]Corresponding author: szyndler@b-tu.de

Abstract

The main aim of the presented research is the analysis of damage evolution in 16MnCrS5 steel during hot forming based on results obtained from finite element modelling. Particular attention is put on the interaction between dynamic recrystallization (DRX) and damage initiation at the matrix-inclusion interface. Moreover, a modified Gurson-Tvergaard-Needleman (GTN) model is proposed with the nucleation criterion taken from an extended Horstemeyer model, which predicts damage nucleation based on material softening due to the DRX and stress state in the material.

Key words: Damage, Dynamic recrystallization, Void nucleation, Numerical modelling

1. INTRODUCTION

Hot forming of metals is commonly used in the industry to produce semi-finished and finished products. It enables to lower the loads needed for the forming operation due to the reduction in yield stresses. Hot forming conditions also improve the material quality at the microscale because of the grain refinement due to recrystallization (Madej, et al., 2016). During hot forming, the ductility, toughness and material strength are improved (Muszka et al., 2014). Also, high temperature enables diffusion processes, which can remove/reduce chemical inhomogeneity (Pietrzyk & Kuziak, 2012; Milenin et al., 2017). In addition, the hot forming enables to reduce unavoidable casting defects, such as porosity (Saby et al., 2015). Unfortunately, the casting process also introduces non-metallic inclusions (impurities) into the material volume, which can cause damage (figure 1) during later hot forming, i.e. rolling (Malkiewicz & Rudnik, 1963; Ervasti & Stahlberg, 2005). Such inclusions, depending on their type, can behave differently during hot forming. They can be rigid or deform with the matrix (Ervasti & Stahlberg, 2005).

Different investigations regarding the influence of non-metallic inclusions on material damage were performed in the past. Most of the literature focuses on experimental analysis of damage in cold forming (Requena et al., 2014; Aşık et al., 2019) and modelling of the observed phenomena (Requena et al., 2014; Liu et al., 2018; Tang et al., 2017; Santos et al., 2018). Only a limited amount of references focuses on damage in hot forming processes (Luo, 2001; Cheng et al., 2017).

Thus, the aim of this work is to analyse the evolution of damage during hot forming, including several phenomena that interact and influence the damage behaviour. Primarily, an interaction between the dynamic recrystallization and damage initiation and propagation at the matrix-inclusion-interface is numerically analysed in the paper.

 ISSN 1641-8581

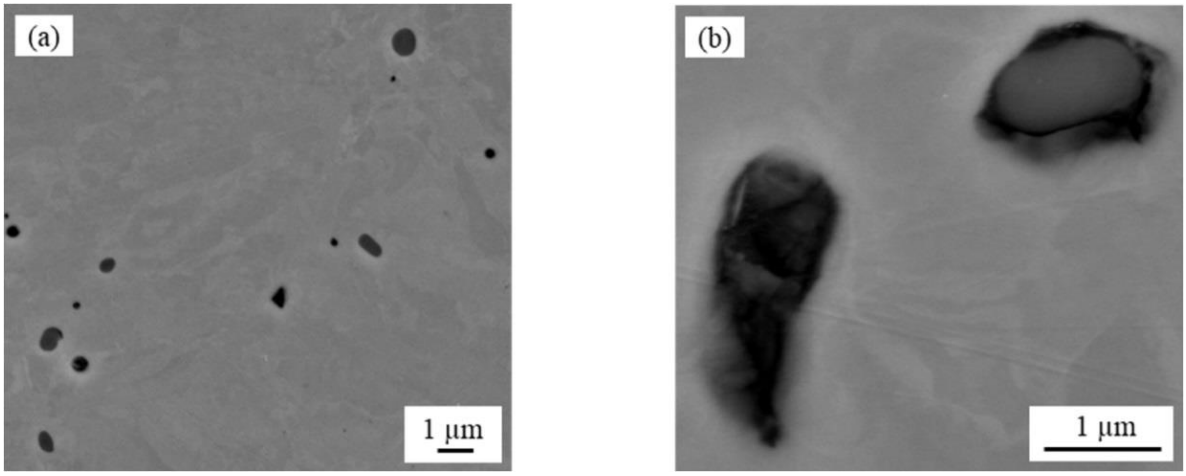

Fig. 1. *Examples of the de-cohesion of steel matrix from the inclusion after material deformation.*

2. FINITE ELEMENT MODEL FOR DAMAGE EVOLUTION

An axisymmetric numerical model, representing the material matrix with a non-metallic inclusion, was developed in Abaqus. The inclusion diameter is 4.25 μm and covers the biggest inclusion size present in the investigated material. To avoid the influence of matrix size on the quality of obtained results, the matrix size is 10 times larger than the inclusion diameter. To simulate the damage evolution during deformation, temperature-dependent cohesive zone elements are located between the matrix and inclusion. The cohesive elements thickness is set to 0.01μm. The matrix and inclusion are discretized with 4-node bilinear axisymmetric elements (CAX4R) and the cohesive zone is meshed with 4-node axisymmetric cohesive elements (COHAX4). An illustration of the Representative Volume Element (RVE) is presented in figure 2.

In the current investigation, the inclusion is modelled as a rigid body, while the matrix has elastoplastic material properties. The matrix is assumed as an isotropic solid with a hardening model that considers dynamic recrystallization.

2.1 Dynamic recrystallization model

The average flow stress in the matrix is based on the model due to Beynon and Sellars equations, which simulate the softening of the matrix due to dynamic recrystallization during the deformation (Beynon & Sellars, 1992):

$$\sigma = \begin{cases} \sigma_0 + (\sigma_{ss0} - \sigma_0)[1 - \exp(-\mathrm{C}\,\varepsilon)]^m, & \varepsilon < \varepsilon_{cr} \\ \sigma_0 + (\sigma_{ss0} - \sigma_0)[1 - \exp(-\mathrm{C}\,\varepsilon)]^m - (\sigma_{ss0} - \sigma_{ss1})\,X, & \varepsilon \geq \varepsilon_{cr} \end{cases} \quad (1)$$

$$\sigma_0 = A_1 \sinh^{-1}\left[\left(\frac{Z}{A_2}\right)^{A_3}\right] \quad (2)$$

$$X = 1 - exp\left[-k'\left(\frac{\varepsilon - \alpha\varepsilon_p}{\varepsilon_p}\right)^{m'}\right] \quad (3)$$

$$\varepsilon_p = A_4 Z^q \quad (4)$$

$$\varepsilon_{cr} = \alpha\,\varepsilon_p \quad (5)$$

$$\sigma_{ss0} = A_5 \sinh^{-1}\left[\left(\frac{Z}{A_6}\right)^{A_7}\right] \quad (6)$$

$$\sigma_{ss1} = A_8 \sinh^{-1}\left[\left(\frac{Z}{A_9}\right)^{A_{10}}\right] \quad (7)$$

$$Z = \dot{\varepsilon}\,\exp\left(\frac{Q}{RT}\right) \quad (8)$$

where: X – recrystallized volume fraction, σ_0, σ_{ss0}, σ_{ss1}, – deformation dependent stresses, Z – Zener-Hollomon parameter, $\dot{\varepsilon}$ – deformation strain rate, Q – activation energy, R – molar gas constant, T - deformation temperature, A_1- A_{10}, α, m', k', p, q - material constants, ε_p – peak strain, ε_{cr} - critical strain.

This model was implemented in FORTRAN as UHARD subroutine. The parameters of this flow stress model are fitted by inverse analysis to experimental data obtained from compression tests performed under five temperatures (800 – 1200°C) and 3 strain rates (0.01, 0.1, 1.0 s^{-1}). Examples of fitted curves for two temperatures and two strain rates are presented in figure 3.

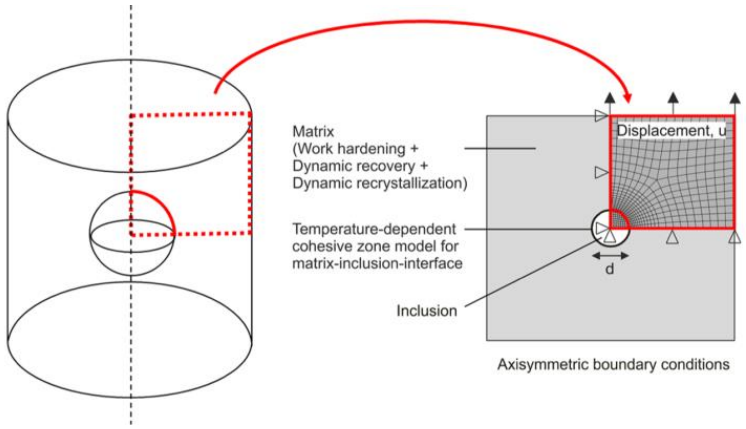

Fig. 2. *Scheme of the developed numerical model in Abaqus software.*

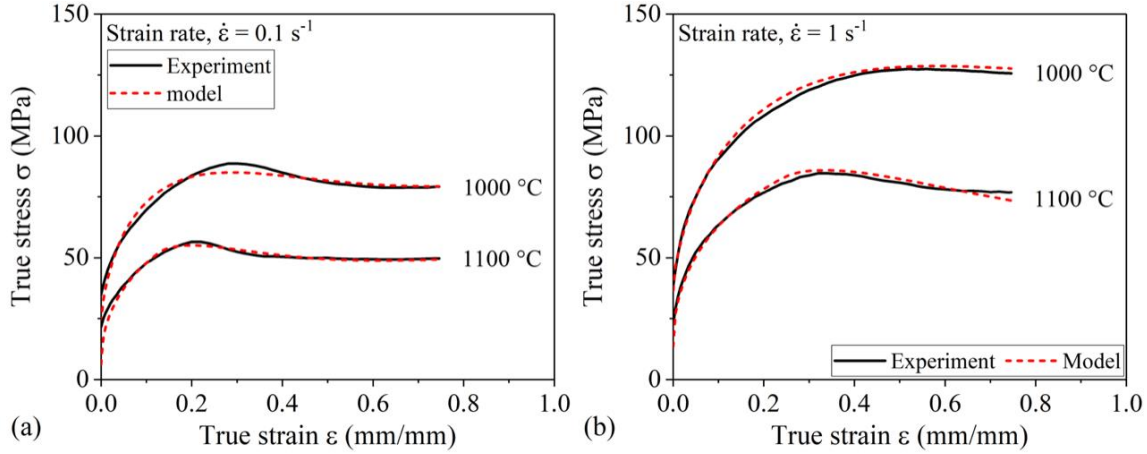

Fig. 3. *Comparison between flow curves calculated with the Beynon - Sellars model and experimental data obtained at strain rates equal to a) 0.1 s^{-1}, b) 1 s^{-1} at temperature 1000°C and 1100°C.*

The RVE model was used to analyze the influence of the temperature, strain rate and total strain on the damage propagation at the inclusion-matrix-interface under the tensile deformation conditions in a vertical direction. The damage is considered as the de-cohesion or void formation at the interface between the steel matrix and the inclusion. The results obtained after 30% deformation are presented in figure 4 in the form of a damage-deformation plot

As can be observed, at constant temperatures of 1000°C and 1100°C, an increase in strain rate from 0.1 s^{-1} to 1 s^{-1} rises the damage value by a factor of 2 and 12, respectively. When the strain rate is constant, a higher temperature (1100°C) reduces the damage value: 15 times for the strain rate of 0.1 s^{-1}, and 2.5 times at for the strain rate of 1 s^{-1}. Thus, to minimize the amount of the damage in a hot formed material, higher temperature and lower strain rate are recommended. Further results present the correlation between the damage and the stress distribution obtained in the deformed matrix at two temperatures and two strain rates (figure 5).

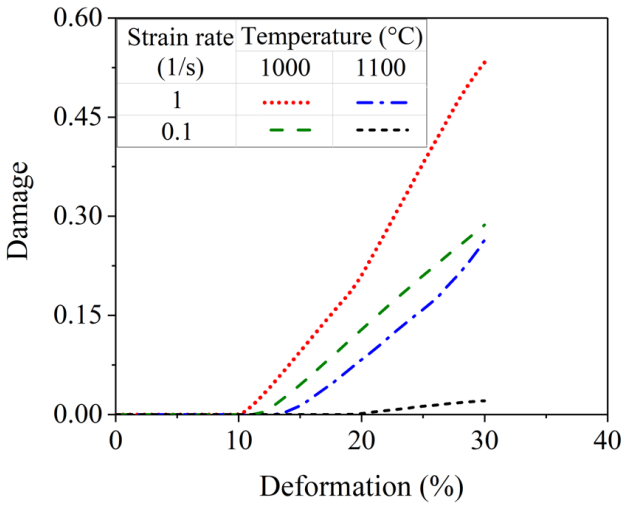

Fig. 4. *The damage nucleation and propagation plots at two temperatures (1000°C, 1100°C) and at two strain rates (0.1 s^{-1}, 1 s^{-1}).*

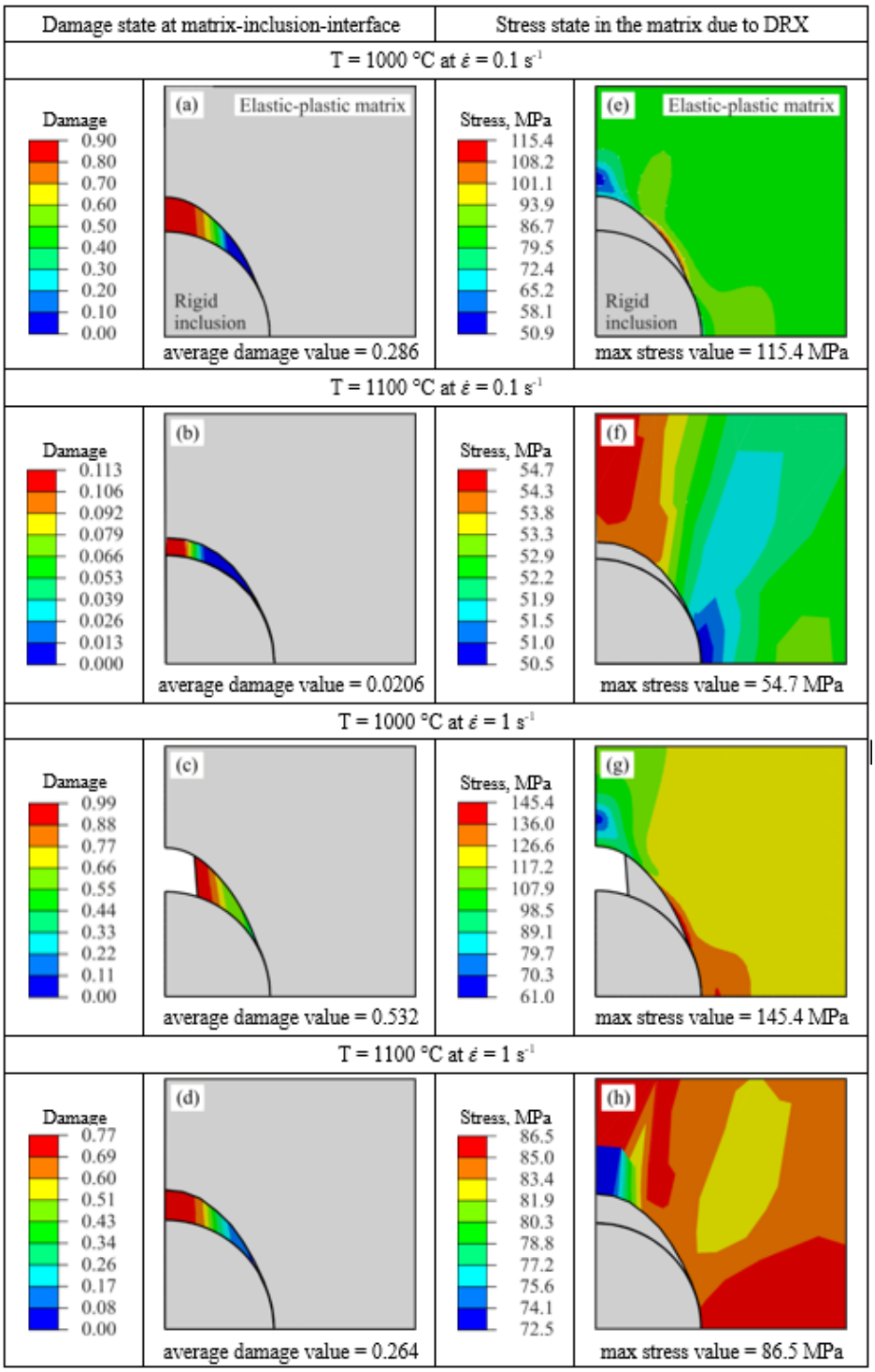

Fig. 5. *The damage and stress distribution in the matrix after deformation at a, e)1000°C and 0.1 s^{-1}; b, f) 1100°C and 0.1 s^{-1}; c, g) 1000°C and 1 s^{-1}; d, h) 1100°C and 1 s^{-1}.*

Obtained results show, that the amount of average damage is proportional to the value of maximum stress present in the matrix during the deformation (figure 5). This analysis proves how important taking into account the material softening due to DRX is. As is visible, the recrystallization phenomenon has a big influence on the stress values in the matrix, which is then strongly influencing the amount of calculated damage in the material. Thus, trials of damage prediction by using FE models should not neglect DRX occurrence. However, not only the stress state of the matrix can have an influence on the damage behavior during hot forming process, but also nucleation of new voids, their growth and merging between existing ones can affect the final amount of the calculated damage in the material.

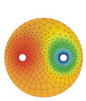

Thus, to model damage in a hot forming process, a model initially proposed by Horstemeyer is adapted, which enables to predict void nucleation during material forming (Horstemeyer & Gokhale, 1999).

2.2 Modification of Horstemeyer's model

Horstemeyer's model takes into account the fracture toughness of the aggregate material, the inclusion size, the strain rate, the initial volume fraction of the inclusions and the stress states for the prediction of damage. The stress state is defined by the triaxiality and the Lode angle, which are assumed to control the void growth and shape change because of damage. The disadvantage of the original Horstemeyer model is that it does not consider the dependence between the damage and flow stress of the matrix. Consequently, the material softening due to the dynamic recrystallization is not taken into account and the model in the original form can be used for cold forming purposes only. Thus, a modified formulation of the Horstemeyer model is proposed, which takes into account the influence of DRX on void nucleation and growth during hot forming:

$$\dot{N} = \frac{\sigma_{DRX}\,\dot{\varepsilon}\sqrt{d}}{K_{IC} f^{1/3}} N \left\{ a' \left(\frac{4}{27} - \frac{J_3^2}{J_2^3} \right) + b' \frac{J_3}{J_2^{3/2}} + c' \frac{I_1}{\sqrt{J_2}} \right\} \tag{9}$$

where: σ_{DRX} – flow stress calculated regarding the DRX (equations 1-8), N - number of voids per unit volume, $\dot{\varepsilon}$ - strain rate, d - inclusion size, K_{IC} - fracture toughness, f - initial volume fraction of inclusions. a', b', c' - material constants. The ratios $J_3/J_2^{3/2}$) and $I_1/\sqrt{J_2}$ account for the Lode parameter and stress triaxiality, respectively.

Based on the proposed model, the damage evolution is calculated from the ratio of the volume of nucleated voids to the total volume of the material at the current state. The damage is initiated, when the volume of the nucleated voids reaches a critical value that corresponds to the critical stress value of the damage initiation:

$$D = \begin{cases} 0 & \text{for } \sigma < \sigma_c \\ \dfrac{N v_v}{1 + N v_v} & \text{for } \sigma \geq \sigma_c \end{cases} \tag{10}$$

Where: v_v - the average void volume is calculated from (Horstemeyer & Gokhale, 1999):

$$\dot{v}_v = \sinh\left(0.001 \frac{\sigma_H}{\sigma_{eff}} \right) \tag{11}$$

Here, σ_H is the hydrostatic stress and σ_{eff} is the von Mises stress. The parameters for the modified Horstemeyer model were identified using the RVE model (figure 6a): d = 4.25 μm, K_{IC} = 71 MPa$\sqrt{\text{m}}$, f = 0.0008, a' = 1.2, b' =0.01, c' =5.89. The proposed model with the parameters identified from the RVE tests is used to predict the void nucleation during the deformation in hot forming conditions at two temperatures and two strain rates (figure 6b).

As can be observed, for higher strain rate, a higher number of voids per unit volume is obtained during the deformation. When the influence of the temperature is investigated, it is observed that with higher temperature less voids per unit volume are initiated. Thus, to maintain damage at the smallest possible level, a higher temperature and the lower strain rate should be applied.

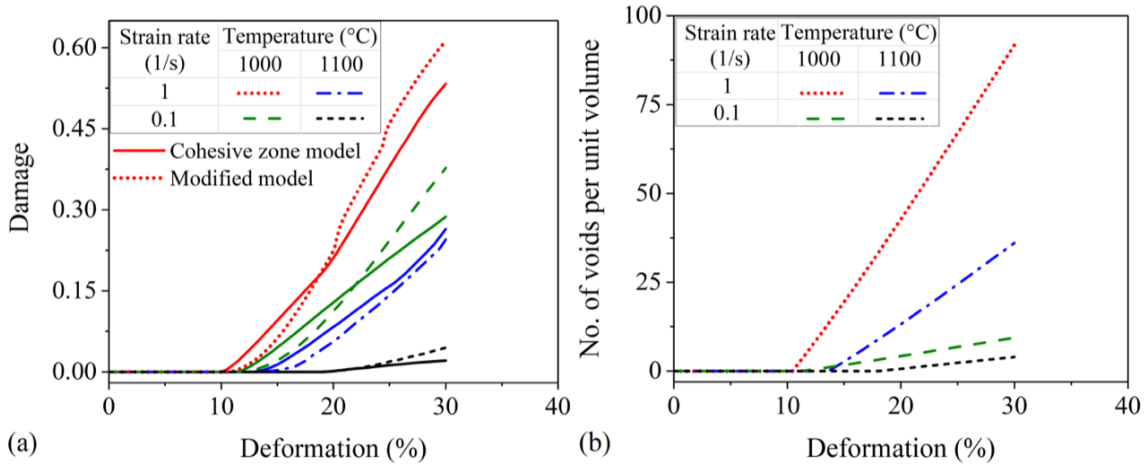

Fig. 6. *Evolution of the a) damage and b) void nucleation at the interface between matrix and inclusions at temperature 1000°C, 1100°C and strain rate 0.1 s^{-1}, 1 s^{-1}.*

The present results showed that it is possible to predict nucleation of voids at the matrix-inclusion interface based on a model that can be integrated into macroscopic finite element simulations. To use this information to calculate the yield stress of the matrix, the damage initiation criterion is integrated into the Gurson-Tvergaard-Needleman (GTN) model.

2.3 Gurson-Tvergaard-Needleman model modification

To couple information about damage with the yield stress during the numerical simulation, the classical Gurson-Tvergaard-Needleman damage model (Gurson, 1977; Tvergaard & Needleman, 1984) was modified using the void nucleation criterion obtained from the modified Horstemeyer model. The GTN yield criterion is:

$$\Phi = \frac{\sigma_v^2}{\sigma_y^2} + 2q_1 f^* \cosh\left(\frac{3q_2\sigma_H}{2\sigma_y}\right) - \left(1 + q_3 f^{*2}\right) \qquad (12)$$

Where: σ_v - the von Mises equivalent stress, σ_y - the initial yield stress, σ_H - the hydrostatic stress, q_1, q_2, q_3, - constitutive parameters, f^{*2} - a damage parameter given by:

$$f^* = \begin{cases} f & \text{for} \quad f < f_c \\ \dfrac{1}{q_1} - f_c & \\ f_c + \dfrac{\frac{1}{q_1} - f_c}{f_f - f_c}\left(f - f_c\right) & \text{for} \quad f > f_c \end{cases} \qquad (13)$$

$$f = f_{nucleation} + f_{growth} \qquad (14)$$

Here, f_c is the critical void volume fraction, f_f the void volume fraction at fracture, $f_{nucleation}$ the void volume fraction due to the nucleation and f_{growth} the void volume fraction due to the growth. In the current investigation, $f_{nucleation}$ value is calculated based on the equation (9):

$$\dot{f}_{nucleation} = \dot{N} = \sigma_{DRX} \frac{\dot{\varepsilon}\sqrt{d}}{K_{IC} f^{1/3}} N \left\{ a' \left(\frac{4}{27} - \frac{J_3^2}{J_2^3} \right) + b' \frac{J_3}{J_2^{3/2}} + c' \left\| \frac{I_1}{\sqrt{J_2}} \right\| \right\} \qquad (15)$$

Parameters of the modified GTN model are fitted to the experimental data obtained from tensile tests performed at 4 temperatures (900–1200°C) and 3 strain rates (0.01, 0.1, 1.0 s^{-1}). The sample dimensions before deformation are presented in figure 7a. The results in form of force-elongation plots were used to identify the parameters of the modified GTN model. Parameter identification was performed in the Abaqus software, where the tensile test was replicated and the modified GTN model parameters were fitted (f_c = 0.2, f_f = 0.3, q_1 = 0.5, q_2 = 1, q_3 = 0.25). Examples of fitted curves for 2 temperatures and 2 strain rates are presented in figure 7.

The proposed modification of the GTN model enables to predict void nucleation considering the material softening due to DRX under hot forming conditions. In figure 8, the evolution of the void volume fraction is presented. VVFN denotes the void nucleation term and VVF nucleation and growth.

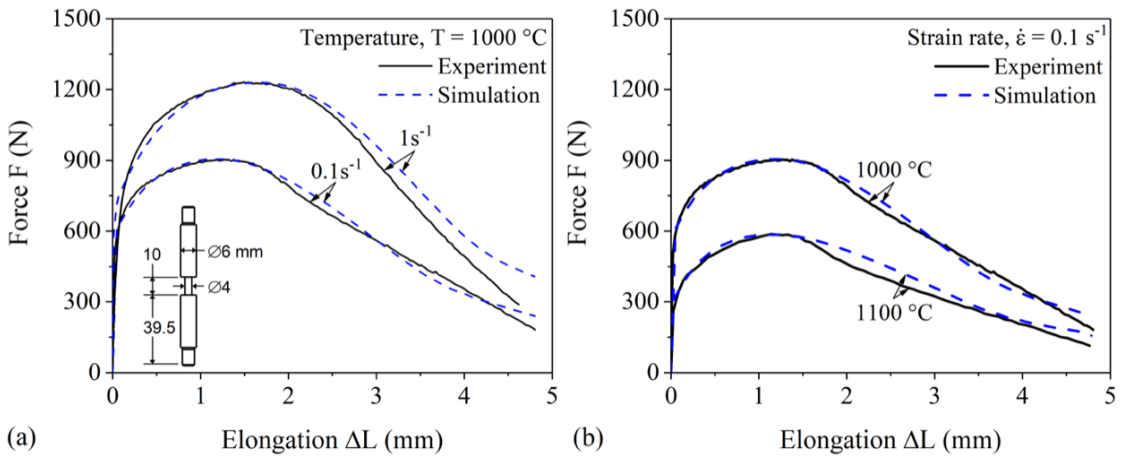

Fig. 7. *Comparison between flow curves calculated with the modified GTN model and experimental data obtained at a) 0.1 s^{-1} and 1 s^{-1} at 1000°C, b) 1000 °C and 1100°C at 0.1 s^{-1}.*

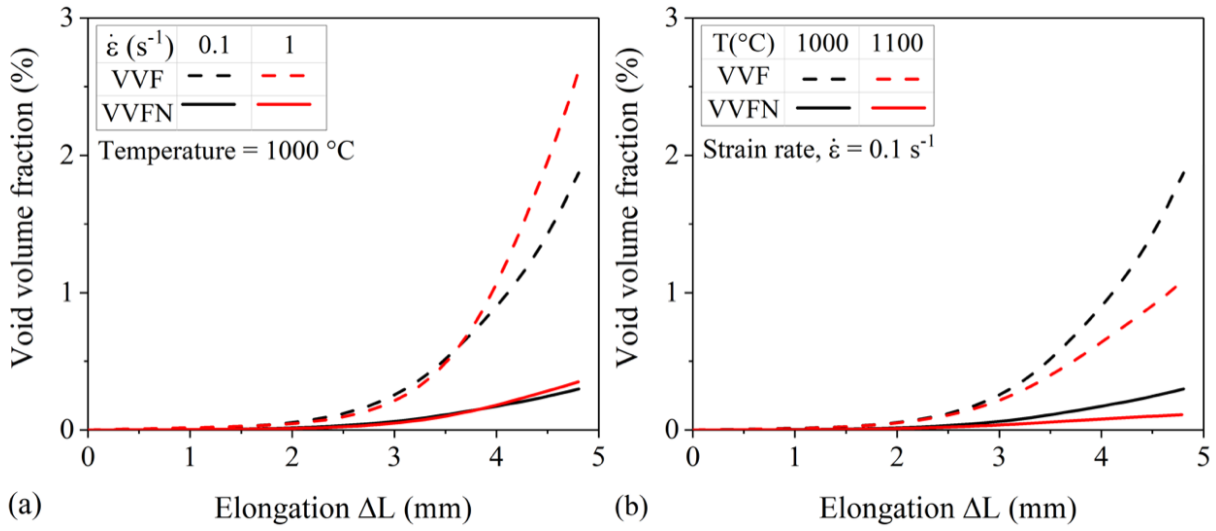

***Fig. 8**. Void volume fraction evolution for a) temperature 1000°C at strain rates 0.1 s^{-1}, 1 s^{-1}, b) strain rate 0.1 s^{-1} at temperatures 1000°C, 1100°C.*

As is visible, the strain rate has legible influence on the VVFN curve at constant temperature. The difference starts when the VVF model is used for elongation above 3.5 mm (figure 8a). Then a higher void volume fraction values appear at the higher strain rate. As expected, a significant difference is noticed in results between models that take into account the void growth. For example, for the strain rate 0.1 s^{-1}, the difference between VVFN and VVF is fourfold and for the strain rate 1 s^{-1} it is even higher (figure 8a). When a constant strain rate is investigated, a larger difference is recognized in both cases (figure 8b). The higher temperature causes a lower void volume (figure 8b).

3. SUMMARY

In the paper, a coupled DRX-damage modelling approach for hot forming processes is proposed. This model is designed for numerical analysis of hot forming processes that include the influence of DRX on void nucleation and growth. The main attention is put on the interaction between dynamic recrystallization and damage initiation. To consider this interaction, the Gurson-Tvergaard-Needleman model was modified with the nucleation criterion taken from the modified Horstemeyer model.

The results presented in the paper enable to draw the following main conclusions:

- a higher temperature causes lower stresses in the matrix resulting in lower damage at the matrix-inclusion interface
- a lower strain rate enables to delay the damage process
- the lowest damage can be obtained by maintaining higher temperature and lower strain rate at the same time
- to reduce appearance of new voids and their growth, high temperature and low strain rate should be kept.

ACKNOWLEDGMENTS

Financial support from German Research Foundation based on the framework of the Transregional Collaborative Research TRR188 “Damage Controlled Forming Processes”, project C03 “Damage modeling during hot forming”. The quantitative data of inclusions were delivered by the Central Facility for Electron Microscopy, Aachen (Germany). Hot compression test were realized at the Institute of Metal Forming, Aachen (Germany). The basic code for GTN model was provided by Institute of Forming Technology and Lightweight Construction, Dortmund (Germany).

REFERENCES

Aşık, E.E., Perdahcıoğlu, E.S., van den Boogaard, A.H., 2019, Microscopic investigation of damage mechanisms and anisotropic evolution of damage in DP600, *Materials Science and Engineering A*, 739, 348-356.

Beynon, J.H., Sellars, C.M., 1992, Modelling microstructure and its effects during multipass hot rolling, *ISIJ International*, 32, 3, 359-367.

Cheng, R., Zhang, J., Wang, B., 2017, Deformation behavior of MnO13%-Al 2 O 3 18%-SiO 2 69% inclusion in different steels during hot rolling processes, *Metallurgical Research Technology*, 114, 608.

Ervasti, E., Stahlberg, U., 2005, Void initiation close to a macro-inclusion during single pass reductions in the hot rolling of steel slabs: A numerical study, *Journal of Materials Processing Technology*, 170, 1-2, 142-150.

Gurson, A.L., 1977, Continuum theory of ductile rupture by void nucleation and growth: part I – yield criteria and flow rules for porous ductile media, *Journal of Engineering Materials and Technology*, 99, 1, 2-15.

Horstemeyer, M.F., Gokhale, A.M., 1999, A void-crack nucleation model for ductile metals, *International Journal of Solids and Structures*, 36, 5029-5055.

Liu, Y., Zhu, Y., Oskay, C., Hu, P., Ying, L., Wang, D., 2018, Experimental and computational study of microstructural effect on ductile fracture of hot-forming materials, *Materials Science & Engineering A*, 724, 298-323.

Luo, C., 2001, Evolution of voids close to an inclusion in hot deformation of metals, *Computational Materials Science*, 21, 360-374.

Madej, Ł., Sitko, M., Pietrzyk, M., 2016, Perceptive comparison of mean and full field dynamic recrystallization models, *Archives of Civil and Mechanical Engineering*, 16, 4, 569-589.

Malkiewicz, T., Rudnik, S., 1963, Deformation of non-metallic inclusions during rolling of steel, *Journal of the Iron and Steel Institute*, 201, 33-38.

Milenin, A., Pernach, M., Rauch, Ł., Kuziak, R., Zygmunt, T., Pietrzyk, M., 2017, Modelling and optimization of the manufacturing chain for rails, *Procedia Engineering*, 207, 2101-2106.

Muszka, K., Dziedzic, D., Madej, L., Majta, J., Hodgson, P.D., Palmiere, E.J., 2014, The development of ultrafine-grained hot rolling products using advanced thermomechanical processing, *Material Science & Engineering A*, 610, 290-296.

Pietrzyk, M., Kuziak, R., 2012, Modelling phase transformation in steel, Woodhead Publishing Series in Metals and Surface Engineering, 145-179.

Requena, G., Maire, E., Leguen, C., Thuillier, S., 2014, Separation of nucleation and growth of voids during tensile deformation of dual phase steel using synchrotron microtomography, *Materials Science & Engineering A*, 589, 242-251

Saby, M., Bouchard, P.-O., Bernacki, M., 2015, Void closure criteria for hot metal forming: A review, *Journal of Manufacturing Processes*, 19, 239-250.

Santos, R.O., Silveira, L.B., Moreira, L.P., Cardoso, M.C., Silva, F.R.F., 2018, Damage identification parameters of dual-phase 600-800 steels on experimental void analysis and finite element simulations, *Journal of Materials Research and Technology*, in press.

Tang, J., Hu, W., Meng, Q., Sun, L., Zhan, Z., 2017, A novel two-scale damage model for fatigue damage analysis of transition region between high- and low-cycle fatigue, *International Journal of Fatigue*, 105, 208-218.

Tvergaard, V., Needleman, A., 1984, Analysis of the cup-cone fracture in a round tensile bar, *Acta Metallurgica*, 32, 157-169.

NUMERYCZNA ANALIZA MIKROUSZKODZEŃ W STALI PODCZAS FORMOWANIA NA GORĄCO

Streszczenie

Analiza numeryczna rozwoju mikrouszkodzeń w stali 16MnCrS5 w trakcie przeróbki plastycznej na gorąco jest tematem niniejszej publikacji. Szczególną uwagę zwrócono na związki mechanizmu odbudowy mikrostruktury w trakcie rekrystalizacji dynamicznej i inicjalizacji oraz propagacji mikrouszkodzeń w bezpośrednim sąsiedztwie wtrąceń niemetalicznych. W trakcie badań wykorzystano model Gursona-Tvergaarda-Needlemana zmodyfikowany o kryterium powstawania mikrouszkodzeń Horstemeyera. W rezultacie uzyskano możliwość określenia ewolucji mikrouszkodzeń podczas odkształcenia z uwzględnieniem rekrystalizacji dynamicznej i jej wpływu na stan naprężenia.

Received: September 23, 2018.
Received in a revised form: November 15, 2018.
Accepted: December12, 2018.